

# Gaseous pollutants in Beijing urban area during the heating period 2007–2008: variability, sources, meteorological, and chemical impacts

W. Lin<sup>1,4</sup>, X. Xu<sup>1</sup>, B. Ge<sup>2</sup>, and X. Liu<sup>3</sup>

<sup>1</sup>Key Laboratory for Atmospheric Chemistry, Centre for Atmosphere Watch & Services, Chinese Academy of Meteorological Sciences, Beijing 100081, China

<sup>2</sup>LAPC/NZC, Institute of Atmospheric Physics, Chinese Academy of Science, Beijing 100029, China

<sup>3</sup>Wuhan Central Meteorological Observatory, Wuhan 430074, China

<sup>4</sup>CMA Meteorological Observation Centre, Beijing 100081, China

Received: 17 February 2011 – Published in Atmos. Chem. Phys. Discuss.: 1 March 2011

Revised: 8 June 2011 – Accepted: 12 July 2011 – Published: 10 August 2011

**Abstract.** Gaseous pollutants,  $\text{NO}_y/\text{NO}_x$ ,  $\text{SO}_2$ , CO, and  $\text{O}_3$ , were measured at an urban site in Beijing from 17 November 2007 to 15 March 2008. The average concentrations (with  $\pm 1\sigma$ ) of NO,  $\text{NO}_2$ ,  $\text{NO}_x$ ,  $\text{NO}_y$ , CO,  $\text{SO}_2$ , and  $\text{O}_3$  were  $29.0 \pm 2.7$  ppb,  $33.7 \pm 1.4$  ppb,  $62.7 \pm 4.0$  ppb,  $72.8 \pm 4.5$  ppb,  $1.99 \pm 0.13$  ppm,  $31.9 \pm 2.0$  ppb, and  $11.9 \pm 0.8$  ppb, respectively, with hourly maxima of 200.7 ppb, 113.5 ppb, 303.9 ppb, 323.2 ppb, 15.06 ppm, 147.3 ppb, and 69.7 ppb, respectively. The concentrations of the pollutants show “saw-toothed” patterns, which are attributable mainly to changes in wind direction and speed. The frequency distributions of the hourly mean concentrations of  $\text{NO}_y$ ,  $\text{SO}_2$ , CO, and  $\text{O}_3$  can all be decomposed in the two Lorentz curves, with their peak concentrations representing background levels under different conditions. During the observation period, the average ratio  $\text{NO}_x/\text{NO}_y$  was  $0.86 \pm 0.10$ , suggesting that the gaseous pollutants in Beijing in winter are mainly from local emissions. Data of  $\text{O}_3$ ,  $\text{NO}_z$ , and  $\text{NO}_x/\text{NO}_y$  indicate that photochemistry can take place in Beijing even in the cold winter period. Based on the measurements of  $\text{O}_3$ ,  $\text{NO}_x$ , and  $\text{NO}_y$ , ozone production efficiency (OPE) is estimated to be in the range of 0–8.9 ( $\text{ppb ppb}^{-1}$ ) with the mean ( $\pm 1\sigma$ ) and median values being  $1.1 (\pm 1.6)$  and 0.5 ( $\text{ppb ppb}^{-1}$ ), respectively, for the winter 2007–2008 in Beijing. This low OPE would cause a photochemical  $\text{O}_3$  source of  $5 \text{ ppb day}^{-1}$ , which is small but significant for surface  $\text{O}_3$  in winter in Beijing.

Downward transport of  $\text{O}_3$ -rich air from the free troposphere is the more important factor for the enhancement of the  $\text{O}_3$  level in the surface layer, while high NO level for the destruction of  $\text{O}_3$ . The concentrations of  $\text{SO}_2$ , CO, and  $\text{NO}_x$  are strongly correlated among each other, indicating that they are emitted by some common sources. Multiple linear regression analysis is applied to the concentrations of  $\text{NO}_y$ ,  $\text{SO}_2$ , and CO and empirical equations are obtained for the  $\text{NO}_y$  concentration. Based the equations, the relative contributions from mobile and point sources to  $\text{NO}_y$  is estimated to be  $66 \pm 30\%$  and  $40 \pm 16\%$ , respectively, suggesting that even in the heating period, mobile sources in Beijing contribute more to  $\text{NO}_y$  than point sources.

## 1 Introduction

Air pollution in cities has caused great concern in many countries. Of particular concern are air pollution problems in the megacities of the world. Beijing is one of the largest cities in China and one of the 25 world megacities, with a resident population of 17.55 million in 2009 (<http://www.bjstats.gov.cn/nj/main/2010-tjnj/index.htm>). Being the political and cultural center of China and having relatively mild climate, Beijing has been very attractive for many people. However, like in many other megacities, the air quality in Beijing has been poor for years and sometimes very bad, endangering human health (Hao et al., 2005, 2007; Shao et al., 2006; Wang et al., 2006). Since the preparation for the Summer Olympics 2008, the situation has been significantly improved after many efforts. Nevertheless, exceedances of air



Correspondence to: X. Xu  
(xuxb@cams.cma.gov.cn)

quality standards can be observed under unfavorable weather conditions.

Emissions related to energy consumption by industry, power plants, domestic heating, and vehicle are the major sources of  $\text{NO}_x$ ,  $\text{SO}_2$ , and other pollutants in Beijing (Hao et al., 2005). It was estimated that about 74 % of the ground level  $\text{NO}_x$  in Beijing is due to vehicular emissions, while power plants and industrial sources contribute only 2 % and 13 %, respectively (Hao et al., 2005). In Beijing, severe air pollution sustained for two or more days was often observed in winter (Li et al., 2007). The ground measurements (Zhang et al., 2006; An et al., 2007, 2008; Liu et al., 2008) and satellite data analyses (Richter et al., 2005; van der A et al., 2008; Zhang et al., 2007b) all show that the concentrations of primary gaseous pollutants in Beijing are much higher in wintertime than in other seasons, which can be attributed to weaker vertical mixing, slower chemical destruction due to the lower temperature, solar radiation, and oxidant levels, and particularly, much higher anthropogenic emissions related to heating in winter. Officially, centralized heating in Beijing usually starts in the middle of November and ends in the middle of the following March. During this period, heating related emission is the major source for  $\text{SO}_2$  and also important source for  $\text{NO}_x$  and CO in the city, particularly its urban area.

Besides the toxicity,  $\text{NO}_x$ ,  $\text{SO}_2$ , and CO are closely related to climate and environment. For example, oxidations of  $\text{NO}_x$  and  $\text{SO}_2$  can produce secondary aerosols and cause acid rain. Photochemical conversion of  $\text{NO}_x$  and CO leads to formation  $\text{O}_3$ , which is a greenhouse gas in the troposphere and toxic for humans and vegetation.  $\text{NO}_x$  is crucial for atmospheric chemistry. The oxidation of  $\text{NO}_x$  can produce other reactive nitrogen oxides, including  $\text{HNO}_3$ ,  $\text{HNO}_2$ , and organic nitrates. The collective name for oxidized forms of nitrogen is total reactive nitrogen oxides ( $\text{NO}_x$  + other reactive nitrogen oxides) and is denoted as  $\text{NO}_y$  (AMS, 2000). Because  $\text{NO}_y$  includes the oxidation products of  $\text{NO}_x$ , it is a more conservative quantity than  $\text{NO}_x$ , hence represents better the pollution extent of reactive nitrogen oxides.

In this study, we present measurements  $\text{NO}_x/\text{NO}_y$ ,  $\text{SO}_2$ , CO, and  $\text{O}_3$  made at an urban site in Beijing during the last heating season before the Summer Olympics 2008 and discuss their variability. We report for the first time  $\text{NO}_y$  measurements in wintertime in Beijing and use the  $\text{NO}_y$  data to obtain  $\text{NO}_z$  ( $\equiv \text{NO}_y - \text{NO}_z$ ), which is further used to determine observation-based ozone production efficiency (OPE). In addition, we show the correlations among the species and some meteorological parameters and investigate the impacts of surface wind and air mass transport on the concentrations of pollutants. Finally, we estimate the relative contributions from point and mobile sources to winter  $\text{NO}_y$  in Beijing urban area.

## 2 Experiment

### 2.1 Observation site

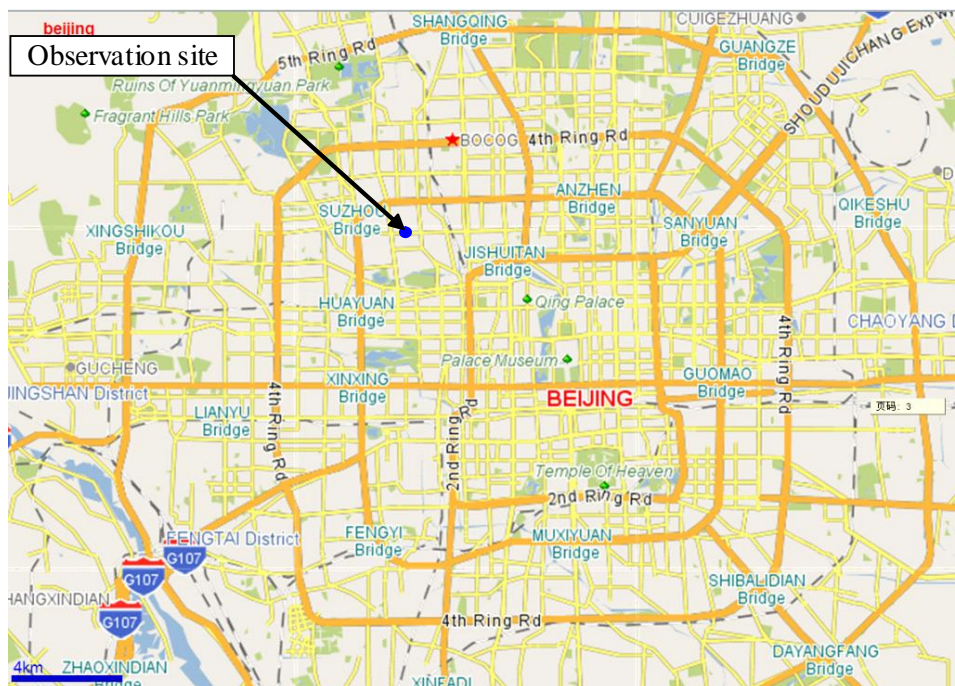
The measurement site (39.95° N, 116.32° E, 96 m a.s.l.) is located in the courtyard of China Meteorological Administration (CMA), Beijing. Figure 1 shows the site location and the traffic network with ring roads and radial arteries. The CMA courtyard is situated in the northwest of the Beijing urban area and between the busy 2nd and 3rd ring roads, with the nearest distances to the 2nd and 3rd ring roads being about 3 km and 1.7 km, respectively. The nearest busy artery, called Zhongguancun Nandajie, is about 450 m to the west.

Figure 2 shows the wind rose and diurnal wind variation during the measurement period (17 November 2007 to 15 March 2008). The prevailing winds were from the NNE and S sectors. About 15.7 % of the measurement time was calm (wind speed  $< 0.3 \text{ m s}^{-1}$ ). The highest and lowest average wind speeds occurred under the NWW and WSW directions, respectively. On diurnal average, the highest wind speed was around 17:00 LT and the lowest one around 06:00 LT. For the average diurnal wind vectors in Fig. 2b, winds from north are dominant during most time of the day except for 16:00–20:00 LT, at which time wind is dominant from west or southwest. There is less precipitation but high-frequency temperature inversion that happens in winter in Beijing.

### 2.2 Instruments and quality control

A set of commercial instruments from Thermo Electron Corporation, USA, were used to measure  $\text{O}_3$  (49C),  $\text{NO}/\text{NO}_2/\text{NO}_x$  (42CTL),  $\text{NO}/\text{NO}_y$  (42CY), CO (48CTL), and  $\text{SO}_2$  (43CTL). A dynamic gas calibrator (Model 146) in combination with a zero air supplier (Model 111) and a standard reference gas mixture ( $\text{SO}_2/\text{NO}/\text{CO}$  in  $\text{N}_2$ ) were used for multipoint calibration and weekly zero/span checks. CO-free air was produced in-situ using the Sofnocat 514 oxidation catalyst (Molecular Products Asia Ltd, Hong Kong) and supplied every 6 h to the CO analyzer for zero drift checks by automatically switching a 3-way solenoid valve. All instruments were housed in an air-conditioned rooftop room of the building (38 m above ground level). An inlet tube (Teflon, 4.8 mm ID  $\times$  8 m length) was shared by the four analyzers except the one for  $\text{NO}_y$ . To minimize the loss of  $\text{NO}_y$  prior to the measurement, an external molybdenum converter module was deployed close to the tube inlet.

Four iterations of multipoint calibrations of CO,  $\text{SO}_2$ ,  $\text{NO}_x$ , and  $\text{NO}_y$  analyzers were made during the observation period. For traceability, the national standard gases of  $\text{SO}_2$ , NO, and CO were compared against NIST-traceable standards from Scott Specialty Gases, USA. Multipoint calibrations of the  $\text{O}_3$  analyzer were made using an  $\text{O}_3$  calibrator (TE 49C PS), which is traceable to the Standard Reference Photometer (SRP) maintained by WMO World Calibration Centre in Switzerland (EMPA).



**Fig. 1.** The location of observation site and the traffic network with ring roads and radial arteries in Beijing (Map from www.bjbus.com).

Measurement signals of trace gases were recorded as 1-min averages. Meteorological data, including wind, temperature, relative humidity, etc., were also obtained from the site, with a resolution of 1 min.

### 3 Results and discussion

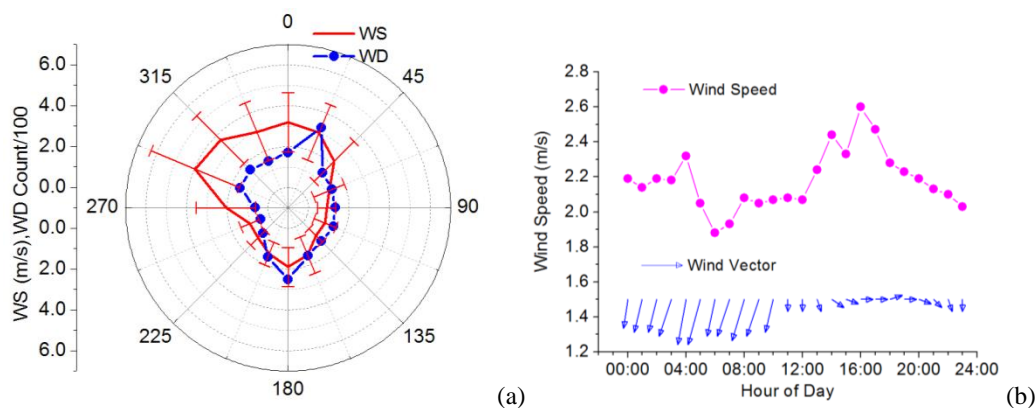
#### 3.1 Concentration levels and variability

Figure 3 shows the time series of hourly average  $O_3$ ,  $SO_2$ , CO, and  $NO_y$  concentrations observed at CMA during the period from 16 November 2007 to 19 March 2008. The 24-h smoothing averages are also plotted in the figure. The concentrations of  $SO_2$ , CO, and  $NO_y$  show “saw-toothed” patterns, indicating that the pollutants concentrations can gradually accumulate to high levels and then decrease sharply to low levels (even close to zero). This is mainly due to the day-to-day variation of atmospheric mixing condition and advection transport. The variation patterns of  $NO_y$ ,  $SO_2$ , and CO seem fairly synchronous, while that of  $O_3$  nearly reversed.

During the whole observation period, NO,  $NO_2$ ,  $NO_x$ ,  $NO_y$ , CO,  $SO_2$ , and  $O_3$  showed overall average (with  $\pm 1\sigma$ ) concentrations of  $29.0 \pm 2.7$  ppb,  $33.7 \pm 1.4$  ppb,  $62.7 \pm 4.0$  ppb ( $99.1 \mu\text{g m}^{-3}$ ),  $72.8 \pm 4.5$  ppb,  $1.99 \pm 0.13$  ppm ( $2.3 \text{ mg m}^{-3}$ ),  $31.9 \pm 2.0$  ppb ( $84.0 \mu\text{g m}^{-3}$ ), and  $11.9 \pm 0.8$  ppb, respectively, and the daily average levels of these gases peaked at 129.6 ppb, 81.0 ppb, 210.5 ppb, 234.8 ppb, 8.71 ppm, 97.6 ppb, and 31.7 ppb, respectively.

Compared with the monitoring data ( $SO_2$ :  $375 \mu\text{g m}^{-3}$ ;  $NO_x$ :  $321 \mu\text{g m}^{-3}$ ; CO:  $5.4 \text{ mg m}^{-3}$ ) in the heating season of 1997 at Chegungzhuang (a site about 2.2 km south of CMA, run by Beijing Municipal Environmental Protection Bureau, <http://www.bjepb.gov.cn>), the primary pollutants had greatly decreased, demonstrating the effectiveness of a series of emission reduction measures implemented during the decadal period before. The average CO concentration (1.99 ppm) is lower than that (2.86 ppm) in winter 2004–2005 reported by An et al. (2008). The concentrations of  $SO_2$  and  $NO_x$  are very close to that in winter 2004–2005 (An et al., 2007) and that in winter 2006 in Beijing (Liu et al., 2008). The observed levels of primary pollutants in winter are higher than those at the polluted rural site Gucheng, 110 km southwest of Beijing urban area (Lin et al., 2009) and much higher than those at the background site Shangdianzi, 100 km northeast of Beijing urban area (Lin et al., 2008; Meng et al., 2009).

The low  $O_3$  value in winter, especially at night, can be attributed to the lower temperature, weaker solar radiation, and particularly, the strong destruction of  $O_3$  by chemical titration of NO from much higher emission of  $NO_x$  related to heating in winter (Lin et al., 2008, 2009). Under the observed average NO concentration of 29 ppb and taking the reaction rate of NO with  $O_3$  at 273 K (Atkinson et al., 1997), the destruction rate of  $O_3$  by NO would be about  $33 \text{ ppb h}^{-1}$ . Such high destruction rate can very effectively suppress the increase of  $O_3$  concentration. In fact, a significant negative



**Fig. 2.** Wind rose (a) and average diurnal wind speed and vector (b) during the observation period. The average diurnal wind vectors are vector averages calculated from the wind velocities and directions, while the average diurnal wind speeds are arithmetic averages of wind speeds.

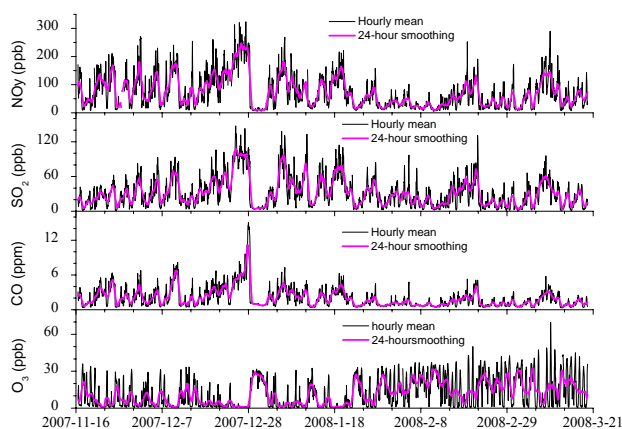


**Fig. 3.** The time series of hourly average  $O_3$ ,  $NO_y$ ,  $SO_2$ , and CO concentrations during the observation period at CMA. The 24-h moving averages are also shown to make the general trends clearer.

correlation between the  $O_3$  and NO concentrations is observed (see Sect. 3.2).

The maximum hourly average concentrations of NO,  $NO_2$ ,  $NO_x$ ,  $NO_y$ , CO,  $SO_2$ ,  $O_3$ , and  $O_x$  were 200.7 ppb, 113.5 ppb, 303.9 ppb, 323.2 ppb, 15.06 ppm, 147.3 ppb, 69.7 ppb, and 137.4 ppb, respectively. No hourly data of  $SO_2$ , CO,  $NO_2$ , and  $O_3$  exceeded the Grade II standard of the Chinese Ambient Air Quality Standards (CAAQS, Revised GB 3095-1996), while the hourly concentrations of  $SO_2$  (>57 ppb),  $NO_2$  (>63.6 ppb), and CO (>8.7 ppm) exceeded the Grade I standard for 480, 195, and 20 h, respectively. About 18 % of the hourly NO data and 39 % of the hourly  $NO_x$  data exceeded 60 ppb, indicating that  $NO_x$  pollution in winter in Beijing was rather severe. For many years,  $SO_2$  was the top gaseous pollutant in Beijing. Reduction of the  $SO_2$  emission and increase in the on-road vehicle number has gradually

changed the situation. The winter level of  $NO_x$  during the winter 2007–2008 was about double as high as that of  $SO_2$ , indicating that  $NO_x$  had been the No. 1 gaseous pollutant.

Figure 4 shows the frequency distributions of hourly average concentrations of  $NO_y$ ,  $SO_2$ , CO, and  $O_3$ . As shown in Fig. 4, the distributions of  $NO_y$ ,  $SO_2$ , and CO have long tails towards the high concentration ends, demonstrating high variability in the concentrations of these species. The distribution of the  $O_3$  concentration is less scattered than those of other gases. To some extent, the peak concentration of each frequency distribution, i.e., the concentration associated with the highest probability, may represent the background level of each pollutant, because the concentration of pollutants at any site and any time depends on the dynamic balance between producing/destroying processes and transport conditions (Lin et al., 2009). However, all the frequency distributions in Fig. 4 show a dominant peak with a sub-peak on its right shoulder, suggesting that some different conditions influenced the pollutants concentrations. In order to differentiate the background levels under different conditions, Lorentz curve fitting was applied to the frequency distributions, and the fitting results are showed in Fig. 4. All distributions can be best fitted using two Lorentzian curves, which can excellently describe the frequency distributions, as implied by the high  $R^2$  values.

For  $O_3$ , CO,  $SO_2$ , and  $NO_y$ , the first curve peaks at 0 ppb, 716 ppb, 5.5 ppb, and 15.6 ppb, respectively, and the second curve peaks at 23.2 ppb, 2130 ppb, 20.4 ppb, and 52.1 ppb, respectively. The large concentration differences suggest that the pollutants concentrations were controlled by two very different atmospheric conditions, as will be discussed in Sect. 3.4. The average concentrations of  $O_3$  and CO lie between the peaks of the respective first and second fitted Lorentzian curves, while those of  $SO_2$  and  $NO_y$  exceed the corresponding peak concentrations of their second fitted Lorentzian curves,

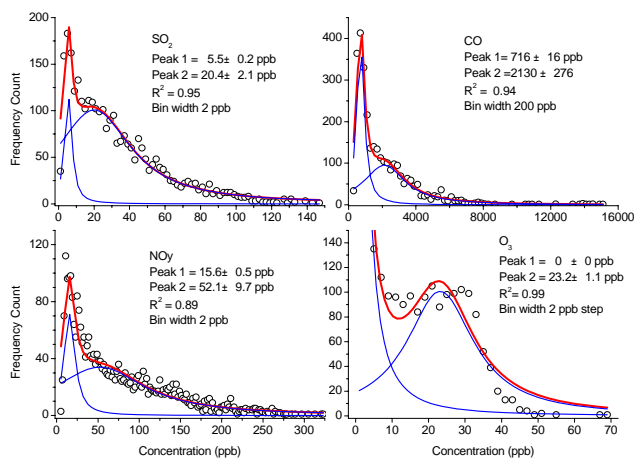


**Fig. 4.** The frequency distributions of hourly average concentrations of  $\text{NO}_y$ ,  $\text{SO}_2$ , CO, and  $\text{O}_3$ . Lorentz curve fitting was applied to the frequency distributions. The large concentration differences between the first and second fitted curves suggest that the pollutants concentrations were controlled by two very different atmospheric conditions.

indicating stronger influences of high pollution events on the concentrations of  $\text{SO}_2$  and  $\text{NO}_y$ . The fact that the first fitted curve of  $\text{O}_3$  peaks at concentration close to zero indicates that surface  $\text{O}_3$  in Beijing is strongly impacted by the gas phase titration reaction of NO with  $\text{O}_3$ , which is particularly effective in lowering the  $\text{O}_3$  level in winter nighttime.

Figure 5 shows the average diurnal variations of CO,  $\text{O}_3$ ,  $\text{SO}_2$ , and  $\text{NO}/\text{NO}_2/\text{NO}_x/\text{NO}_z/\text{NO}_y$  during the observation period. As can be seen in this figure, the  $\text{O}_3$  concentration shows a typical diurnal cycle related to photochemical and dynamic balances, with a maximum (23.1 ppb) around 14:00 LT and minimum (5.8 ppb) around 07:00 LT. During nighttime,  $\text{O}_3$  can be removed by gas titration with high level of NO. This chemical sink caused a very low level of nighttime  $\text{O}_3$  (<8 ppb), but the nighttime NO level (above 30 ppb) was sustained by fresh emission.  $\text{NO}_z$  shows a few ppb higher levels in daytime than in nighttime, indicating greater conversion of  $\text{NO}_x$  in daytime.

The  $\text{SO}_2$ , NO,  $\text{NO}_2$ ,  $\text{NO}_x$ ,  $\text{NO}_y$ , and CO concentrations show similar diurnal patterns with elevated concentration during the night, a peak around 08:00 LT, and a broad valley in the afternoon. The early morning peak is consistent with the rush hour emissions in Beijing urban area (Hao et al., 2000). The large nighttime-afternoon differences should be mainly due to larger emissions from heating in combination with stronger temperature inversion during the nighttime. Stronger removal of the nitrogen-containing species through photochemical reactions during the daytime may play a role as well in the day-night differences. But this should be less important considering the weak intensity of photochemistry in winter. Since mobile sources emit much less  $\text{SO}_2$  than  $\text{NO}_x$  and CO, the morning peak of  $\text{SO}_2$  may

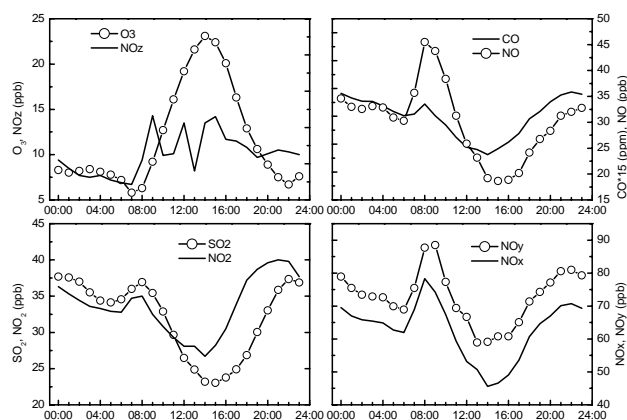


**Fig. 5.** The average diurnal variations of the concentrations of  $\text{O}_3$ ,  $\text{NO}/\text{NO}_2/\text{NO}_z/\text{NO}_x/\text{NO}_y$ , CO, and  $\text{SO}_2$  at CMA in winter. Primary pollutants show similar diurnal patterns which indicate the dominant local emissions. During nighttime,  $\text{O}_3$  is removed substantially by gas titration with high level of NO.

be related to other human activities such as burning of honeycomb coal briquettes for cooking, refueling the coal-burning boilers for heating office buildings, etc. Another explanation for the morning  $\text{SO}_2$  peak is the development of temperature inversion (An et al., 2007). The diurnal pattern of  $\text{SO}_2$  in Beijing urban area looks very different from those observed at Shangdianzi (Lin et al., 2008) and at Gucheng (Lin et al., 2009), the latter ones showed maxima around noon presumably related to long-range  $\text{SO}_2$  transport and vertical mixing.

### 3.2 Concentration ratios and implications to emission sources

To study the relationship among pollutants concentrations and meteorological parameters, Pearson's correlations are calculated from the hourly mean values of the quantities. The obtained correlation coefficients are given in Table 1, together with their significance levels.

In winter, NO,  $\text{NO}_2$ ,  $\text{NO}_x$ ,  $\text{NO}_y$ ,  $\text{NO}_z$ , CO, and  $\text{SO}_2$  are positively and significantly correlated among each other, suggesting that they are dominantly affected by some common factors, for example, emission sources. Wind speed (WS) and  $\text{O}_3$  are positively correlated with each other and negatively correlated with NO,  $\text{NO}_2$ ,  $\text{NO}_x$ ,  $\text{NO}_y$ ,  $\text{NO}_z$ , CO, and  $\text{SO}_2$ . In winter, photochemical reaction is at its weakest. Therefore, the variations of pollutants concentrations depend much more on dynamical processes such as mixing, advection, etc. High wind speed promotes atmospheric mixing, dispersion, and transport, hence favors the dilution of the primary pollutants and transport of  $\text{O}_3$ -richer air from above the inversion layer or from the clean sector. Air temperature is mainly correlated with  $\text{O}_3$  and  $\text{NO}_z$ . The positive correlations agree with the idea that, even in winter, photochemistry in Beijing can still produce certain amounts of

**Table 1.** Pearson's correlation coefficients among gases and meteorological parameters.

	O <sub>3</sub>	CO	SO <sub>2</sub>	NO	NO <sub>2</sub>	NO <sub>x</sub>	NO <sub>z</sub>	NO <sub>y</sub>	WS	T	RH
O <sub>3</sub>	1										
CO	-.571*	1									
SO <sub>2</sub>	-.636*	.805*	1								
NO	-.578*	.860*	.783*	1							
NO <sub>2</sub>	-.746*	.787*	.827*	.751*	1						
NO <sub>x</sub>	-.674*	.886*	.847*	.971*	.887*	1					
NO <sub>z</sub>	-.294*	.616*	.551*	.424*	.619*	.520*	1				
NO <sub>y</sub>	-.655*	.904*	.857*	.944*	.905*	.987*	.649*	1			
WS	.584*	-.458*	-.469*	-.507*	-.521*	-.543*	-.254*	-.531*	1		
T	.229*	-.043**	-.132*	-.083*	.124*	-.014	.273*	.039**	.080*	1	
RH	-.568*	.643*	.550*	.557*	.501*	.570*	.451*	.592*	-.466*	-.248*	1

\* Significant at the 0.01 level; \*\* significant at the 0.05 level.

oxidants. Relative humidity (RH) is positively correlated with NO, NO<sub>2</sub>, NO<sub>x</sub>, NO<sub>y</sub>, NO<sub>z</sub>, CO, and SO<sub>2</sub> and negatively correlated with O<sub>3</sub> and wind speed. High wind speed concurs usually with lower humidity, hence may indirectly cause the above relationships. Although air temperature (*T*) may influence both RH and O<sub>3</sub>, it was not the major factor causing the negative RH-O<sub>3</sub> correlation. As shown in Table 1, the absolute value of the correlation coefficient (*R*) of the WS-RH correlation is much larger than that of the WS-*T* correlation; and the absolute *R* values of the WS-O<sub>3</sub> correlation and the RH-O<sub>3</sub> correlation are much larger than that of the *T*-O<sub>3</sub> correlation. These correlations suggest that RH is more closely linked with WS than with *T*, and that there are closer relationships among WS, RH, and O<sub>3</sub>. Furthermore, daily mean data instead of hourly mean data are used to make the correlations between O<sub>3</sub>, *T*, RH, and WS. This can avoid the influence of the diurnal variations on the correlations. As a result, *T* is not significantly correlated with O<sub>3</sub>, RH, and WS anymore. Therefore, in winter Beijing, wind speed is the main factor indirectly causing the negative correlation of RH with O<sub>3</sub> and the positive correlation of RH with other pollutants. The similar phenomenon is also reported in other papers (e.g., An et al., 2007, 2008; Li et al., 2007; Lin et al., 2009).

In winter when the photochemical transformation becomes much weaker, the variations of the primary pollutants are driven mainly by emission and mixing processes. If the pollutants are emitted by some common sources or co-located sources having similar temporal variations, ambient concentrations of these pollutants will be well correlated among each other after dilution.

To further examine the correlations among primary pollutants and the related factors, data were grouped into subsets representing the whole day, daytime (07:00–18:00 LT), and nighttime (19:00–06:00 LT), respectively, and linear regressions were carried out on each subset of data. Table 2 shows the slopes, intercepts, with their errors, and correlation coef-

ficients (*R*<sup>2</sup>) of the CO-NO<sub>x</sub> (CO-NO<sub>y</sub>) and SO<sub>2</sub>-NO<sub>x</sub> (SO<sub>2</sub>-NO<sub>y</sub>) regression lines for different subsets of data. The differences between the daytime and nighttime slopes are small, but larger than a few times of the errors, suggesting that the slopes of daytime regression lines are significantly different from the nighttime ones. The slopes of daytime regression lines are a little lower than those of the corresponding nighttime regression lines, suggesting that sources of CO and SO<sub>2</sub> is stronger in nighttime than in the daytime, and/or the chemical removal of NO<sub>x</sub> (NO<sub>y</sub>) is more rapid in daytime than in nighttime. More heating demand at night can explain the day-night difference since coal burning emits more SO<sub>2</sub> and CO than NO<sub>x</sub>, therefore the higher nighttime emission factors of SO<sub>2</sub> and CO. The average emission factors of SO<sub>2</sub> and NO<sub>x</sub> from coal burning in Beijing were estimated to be 15.4 and 8.7 kg t<sup>-1</sup> coal, respectively (Hao et al., 2007). Industrial and domestic coal burning in China emits much more CO than NO<sub>x</sub> (Ohara et al., 2007; Zhang et al., 2009).

The slope of the CO-NO<sub>y</sub> regression line in winter in Beijing is smaller than that (36 ppb ppb<sup>-1</sup> in nighttime/winter) obtained at Linan, a rural site in the Yangtze Delta region (Wang et al., 2002) and that (34.6 ppb ppb<sup>-1</sup> in nighttime/winter) obtained at Gucheng, a rural site in the North China Plain (Lin et al., 2009). Biomass burning, which has much higher CO/NO<sub>x</sub> emission ratio than other sources, is proposed to be a major source for the high CO level at the two rural sites. The mean value of all SO<sub>2</sub>/NO<sub>y</sub> data is 0.46 ppb ppb<sup>-1</sup>. The slopes of the CO-NO<sub>y</sub> regression lines for high- (SO<sub>2</sub>/NO<sub>y</sub> > 0.46 ppb ppb<sup>-1</sup>) and low-SO<sub>2</sub> (SO<sub>2</sub>/NO<sub>y</sub> ≤ 0.46 ppb ppb<sup>-1</sup>) are 26 ppb ppb<sup>-1</sup> and 27 ppb ppb<sup>-1</sup>, respectively, suggesting that CO and NO<sub>y</sub> at the CMA site are emitted from some common sources that do not make significant contribution to SO<sub>2</sub>.

The winter nighttime SO<sub>2</sub>/NO<sub>x</sub> ratio for the CMA site, as expressed by the slope (0.43) of the SO<sub>2</sub>-NO<sub>x</sub> regression line, is only about a half of that (0.83 in nighttime/winter) obtained at the Linan background station by Wang et al. (2002).

**Table 2.** The slopes, intercepts, with their errors, and correlation coefficients ( $R^2$ ) values in the regression lines of CO-NO<sub>x</sub>, SO<sub>2</sub>-NO<sub>x</sub>, CO-NO<sub>y</sub>, and SO<sub>2</sub>-NO<sub>y</sub>.

	Slope	Intercept	$R^2$	Slope	Intercept	$R^2$
	(ppb ppb <sup>-1</sup> )	(ppb)		(ppb ppb <sup>-1</sup> )	(ppb)	
	CO-NO <sub>y</sub>			SO <sub>2</sub> -NO <sub>y</sub>		
All data	26.6±0.2	49±22	0.817	0.372±0.004	4.6±0.4	0.734
Daytime	24.1±0.3	117±23	0.844	0.342±0.005	4.4±0.5	0.758
Nighttime	28.9±0.4	-18±35	0.813	0.399±0.006	4.8±0.6	0.731
	CO-NO <sub>x</sub>			SO <sub>2</sub> -NO <sub>x</sub>		
All data	29.3±0.3	147±23	0.785	0.413±0.005	5.7±0.4	0.717
Daytime	27.3±0.3	196±26	0.824	0.388±0.006	5.5±0.5	0.739
Nighttime	30.9±0.5	105±39	0.764	0.432±0.007	6.1±0.6	0.706

This may be attributable to the difference in the emission characteristics between urban and rural areas. The CMA site, being located in a megacity, is much more influenced by vehicle emissions. Lin et al. (2009) obtained a SO<sub>2</sub>/NO<sub>x</sub> ratio of 0.30 for winter nighttime at Gucheng, a rural site 110 km southwest of Beijing. This ratio is slightly lower than that for the CMA site. Since Gucheng is far away from major cities and about 7 km away from the nearest highway, the lower SO<sub>2</sub>/NO<sub>x</sub> ratio is not caused by vehicle emissions but by high contributions from biomass burning (Lin et al., 2009).

Besides common sources, mixing processes may have resulted in highly significant correlations among CO, NO<sub>y</sub>, and SO<sub>2</sub> (Table 2). The very similar behaviors for the CO, NO<sub>y</sub>, and SO<sub>2</sub> concentrations in winter (Fig. 3), particularly the similar patterns, indicate that the variations of these gases in winter in Beijing are strongly influenced by mixing processes (see more details in Sect. 3.4).

### 3.3 Relative contributions of point and mobile sources to NO<sub>y</sub>

Relationships between NO<sub>y</sub>, CO, and SO<sub>2</sub> can provide some information on the emission sources. Usually, mobile sources emit high level of CO but relatively low level of SO<sub>2</sub>, and point sources (mainly coal-burning) emit high level of SO<sub>2</sub> but relatively low level of CO. These two types of sources are the major sources of NO<sub>y</sub>. Therefore, NO<sub>y</sub> may correlate well with both SO<sub>2</sub> and CO. Multiple linear regression analysis is often used to estimate the relative contributions from point and mobile sources to NO<sub>y</sub> (Stehr et al., 2000; Tong et al., 2005).

To investigate the relative contributions from point (stationary) and mobile sources to winter NO<sub>y</sub> in Beijing, an empirical model is created, with NO<sub>y</sub> being the response variable and SO<sub>2</sub> and CO being the explanatory variables. The mathematical expression of the model is

$$[\text{NO}_y] = \alpha[\text{CO}] + \beta[\text{SO}_2] + \delta, \quad (1)$$

where  $\alpha$  and  $\beta$  are the linear coefficients between [NO<sub>y</sub>] and [SO<sub>2</sub>] and [CO], respectively, and  $\delta$  is the intercept.

According to the INTEX-B.v1.2 data (<http://mic.greenresource.cn/intex-b2006>; Zhang et al., 2009), transportation contributes 52 % to CO for the entire area of Beijing and 60 % to CO for the grid (Center at 40° N, 116.5° E with 0.5° × 0.5°) where the CMA site locates. Emissions from stationary sources (industry, power plant, and residential) make a contribution of 38 % to CO for the entire city and 40 % for the CMA grid. About 73 % of SO<sub>2</sub> is emitted from power plant and industry sources both for the entire Beijing and for the CMA grid, and transportation contributes less than 4 % to SO<sub>2</sub>. Emissions of CO from biomass burning in North China (outside Beijing, mainly from south of Beijing because Beijing locates in the north edge of the North China plain) seems insignificant in winter because the prevailing winds in winter are from the north (Fig. 2), the clean sector. Therefore, the major uncertainties associated with the assumption may be from the co-emission of CO and SO<sub>2</sub> by industry and power plant sources, which should be less than 40 %.

Before the parameterization of  $\alpha$  and  $\beta$ , the collinearity effects of SO<sub>2</sub> and CO on the estimates of regression coefficients were diagnosed. The Variance Inflation Factor (VIF) is 2.89 (<10) and the condition index is 5.73 (<30), suggesting that the collinearity is not significant. According to the emission inventories (Zhang et al., 2009), more than 50 % of CO in Beijing is from mobile sources and about 96 % of SO<sub>2</sub> from stationary sources. The great difference in emission sources is consistent with the insignificant co-linearity between CO and SO<sub>2</sub>, which is also suggested by the low VIF value. The insignificant co-linearity seems to be contradictory to the high correlation coefficient for CO-SO<sub>2</sub> (0.805, Table 1). As CO and SO<sub>2</sub> are mainly from the local sources in winter in urban Beijing, the meteorological factors may

**Table 3.** Results of multiple linear regressions of  $\text{NO}_y$  with CO and  $\text{SO}_2$  for different datasets.

Datasets	Fitted models*	$R^2$	Prob>  t
Daytime	$[\text{NO}_y]= (0.024 \pm 0.001)[\text{CO}] + (0.907 \pm 0.040)[\text{SO}_2] + (1.23 \pm 0.85)$	0.885	< 0.0001
Nighttime	$[\text{NO}_y]= (0.019 \pm 0.000)[\text{CO}] + (0.802 \pm 0.032)[\text{SO}_2] + (6.81 \pm 0.86)$	0.865	< 0.0001
All data	$[\text{NO}_y]= (0.021 \pm 0.000)[\text{CO}] + (0.835 \pm 0.027)[\text{SO}_2] + (5.18 \pm 0.66)$	0.862	< 0.0001

\* Unit for all variables: ppb.

exert similar influences on the concentrations of both gases, with wind direction, wind speed (WS), and mixing layer height being the key factors. Table 1 indicates that both CO and  $\text{SO}_2$  are significantly anti-correlated with WS. Figure 6 shows that strong north wind causes extremely low concentrations of both gases. Therefore, the significant correlation between CO and  $\text{SO}_2$  may mainly be caused by similar meteorological impacts rather than by co-linearity between them.

Table 3 presents the multiple linear regression results, showing good correlations of  $\text{NO}_y$  with CO and  $\text{SO}_2$  for the datasets daytime (07:00–18:00 LT), nighttime (18:00–07:00 LT), and all data. T-tests indicate that the correlations are highly significant. On average, the coefficient  $\alpha$  in Beijing for winter 2007–2008 is 0.021, which is lower than most of those reported by Tong et al. (2005). The coefficient  $\beta$  is 0.835, which is higher than those in the Great Smoky Mountain National Park (0.68) and in the Mammoth Cave National Park (0.57), USA, for winter 1995–1998 (Tong et al., 2005), and higher than those at Arendtsville (0.36–0.41), for June–September, and at the Wye site (0.18–0.48), USA, for September–December, but very close to those in the high-elevation Shenandoah National Park (0.75–0.88), USA, for September–December (Stehr et al., 2000). These differences indicate that the emission ratios in Beijing are quite different from those in many areas of USA.

The coefficients  $\alpha$  and  $\beta$  for daytime and nighttime were applied to the calculations of relative contributions of mobile and point sources. For each hourly data, ( $\alpha \cdot [\text{CO}]$ ) and ( $\beta \cdot [\text{SO}_2]$ ) are calculated and then the values are divided by  $[\text{NO}_y]$  to represent the relative contributions of mobile and points sources, respectively. Observations with an absolute studentized residual  $> 2$  were not included in the calculations. On average, the contribution from mobile source was about  $66 \pm 30\%$  (70% for daytime and 62% for nighttime) and the contribution from point source was about  $40 \pm 16\%$  (39% for daytime and 41% for nighttime) to  $\text{NO}_y$  during winter 2007–2008 in Beijing. As the background levels of CO and  $\text{SO}_2$  are negligible compared with the urban level of CO and  $\text{SO}_2$  in winter Beijing urban, they were not excluded in the regression analysis. This treatment, together with statistical uncertainties, may have introduced bias to the final results, causing a total contribution  $> 100\%$ . Interestingly, these results agree fairly well with those reported by Zhang et al. (2007a), who obtained relative contributions of 80%

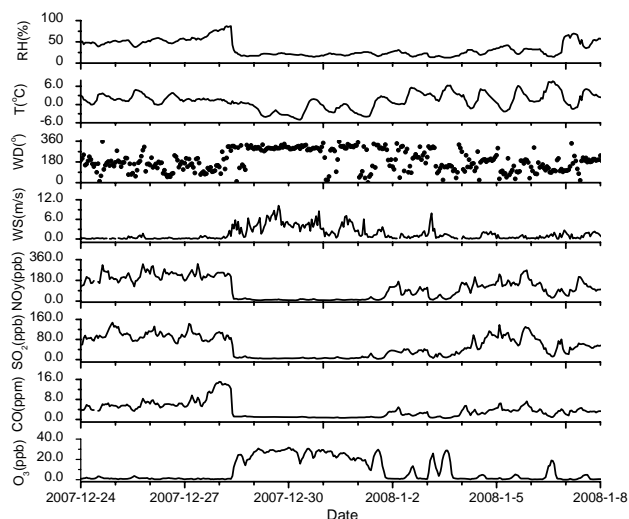


**Fig. 6.** A case for pollutants' accumulation and dilution. From 28 December 2007 to 1 January 2008, the cold, fast-moving air masses, lasting about four days, brought higher  $\text{O}_3$  concentration and facilitated the dilution of local pollutants in Beijing.

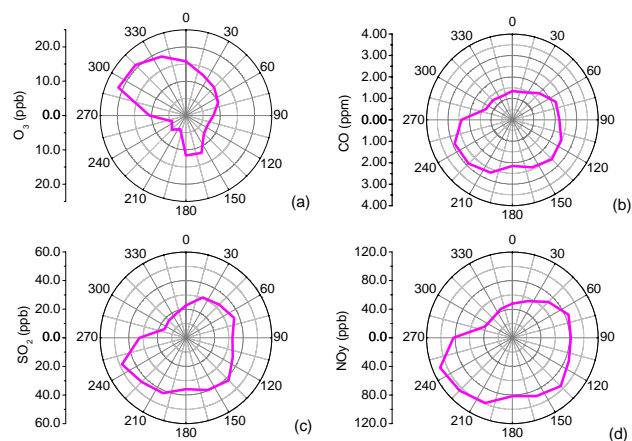
(daytime) and 68% (nighttime) from motor vehicle sources and of 20% (daytime) and 32% (nighttime) from coal combustion sources, respectively, to carbonaceous aerosols in winter Beijing.

On the basis of emission data in 2006 (Zhang et al., 2009), a relative contribution of about 53% to  $\text{NO}_x$  is estimated to be from transportation in the grids encompassing Beijing and about 47% from power, industry, and residential sources. The portion from mobile sources (53%) is a little smaller than that (66%) obtained in this study from the observations. This small discrepancy can be at least qualitatively explained by the changes in emission sources in 2007. For preparation of the Olympic Games 2008, many emission control measures were implemented in Beijing and surrounding areas, so that the emissions from point sources might have been significantly reduced by the winter 2007–2008. In addition, vehicle numbers in Beijing had increased about 20% in 2007, inevitably leading to higher emission of  $\text{NO}_x$  from mobile sources.

### 3.4 Meteorological impacts on pollutant concentrations

The primary air pollutants are generally more diluted with increasing winds and accumulated under weak winds in Beijing, as shown in other studies (e.g., An et al., 2008; Zhang et al., 2007a; Ding et al., 2002; Streets et al., 2007). Figure 6 shows a typical case from 24 December 2007 to 7 January 2008. Primary pollutants accumulated to high levels during a period of air stagnation and then decreased suddenly to low levels on 28 December 2007 and remained low during a 4-day period with strong northerly winds. From 00:00 LT on 24 December 2007 to 08:00 LT on 28 December 2007, the average wind speed was only  $0.3 \text{ m s}^{-1}$ , and the average concentrations of NO, NO<sub>x</sub>, NO<sub>y</sub>, SO<sub>2</sub>, and CO were 118.5 ppb, 193.4 ppb, 219.8 ppb, 96.1 ppb, and 6.99 ppm, respectively, with the maxima of 200.7 ppb, 303.9 ppb, 323.2 ppb, 147.3 ppb, and 15.06 ppm, respectively. From 08:00 LT on 28 December 2007 to 18:00 LT on 1 January 2008, the wind speed averaged  $3.8 \text{ m s}^{-1}$  (with a maximum of  $10.2 \text{ m s}^{-1}$ ) and the concentrations of NO, NO<sub>x</sub>, NO<sub>y</sub>, SO<sub>2</sub>, and CO averaged only 2.1 ppb, 12.0 ppb, 12.8 ppb, 6.7 ppb, and 0.94 ppm, respectively. Due to the strong titration by high level of NO, the O<sub>3</sub> concentration during the first period was very low. From the first to the second period, the average concentration of O<sub>3</sub> increased sharply from 1.1 ppb to 24.2 ppb, the average temperature decreased from  $1.9^\circ$  to  $-1.5^\circ$ , and the average RH decreased from 55 % to 20 %. During the second period, O<sub>3</sub> held high level with small diurnal change. All these phenomena were caused by colder, dryer, and O<sub>3</sub>-richer air rapidly descending to the site. The cold, fast-moving air masses, lasting about four days, brought higher O<sub>3</sub> concentration and facilitated the dilution of local pollutants in Beijing. After this synoptic process, the weather changed to be in favor of pollution accumulation. Therefore, the observed “saw-toothed” patterns of pollutant concentrations (see Fig. 1) are related to the periodic changes of synoptic systems, which have different ability of atmospheric dispersion.

Figure 7 shows the average concentrations of NO<sub>y</sub>, SO<sub>2</sub>, CO, and O<sub>3</sub> for 16 wind direction sectors (clockwise from north). The concentrations of NO<sub>y</sub>, SO<sub>2</sub>, and CO show similar patterns, with higher values from northeast to southwest sectors and lower values from northwest to north sectors. The reverse is true for O<sub>3</sub>. The observation site is located in the northwest quadrant of Beijing urban area. As can be seen in Fig. 1, there are more greenbelts and less roads in the northwest-north sector. Air masses from northwest and north are often cold and dry with features of free atmosphere (high O<sub>3</sub> concentration, low primary pollutants concentrations, and relatively low humidity) and are often associated with high wind speeds (see Fig. 2a). The northwest and north sides of Beijing are surrounded by mountains and the other sides by plains. This kind of topography favors pollutants accumulation under winds from south and east and pollutants dilution under winds from northwest and north.

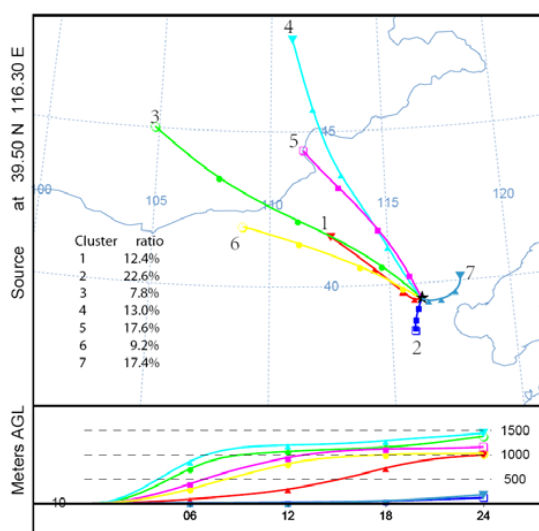


**Fig. 7.** The average concentrations of O<sub>3</sub>, NO<sub>y</sub>, SO<sub>2</sub>, and CO in corresponding wind direction sectors. Strong winds from northwest help the transport of higher ozone level to surface and facilitated the dilution of primary pollutants.

While surface wind direction only gives an insight into the first order advection processes to impact pollutants variability, trajectory analyses are further used to provide the information about the impact of long-range air transport on the surface trace gases. Backward trajectories were calculated using the HYSPLIT4.8 model from NOAA Air Resources Laboratory (<http://www.arl.noaa.gov/ready/hysplit4.html>) and the 6-hourly archive meteorological data from the NCEP Global Data Assimilation System (GDAS) ( $1^\circ \times 1^\circ$ ). The trajectory endpoint is  $39.95^\circ \text{ N}$  and  $116.32^\circ \text{ E}$  with a height of 10 m above the ground level. The 24-h backward trajectories were calculated for four time points (00:00, 06:00, 12:00, 18:00 UTC) per day for the observation period. The individual trajectories were grouped into 7 clusters using the clustering tool included in HYSPLIT4.8. Figure 8 shows the mean trajectories for the 7 clusters and their ratios to the total number of trajectories. Observed trace gas concentrations are associated with the trajectories and then grouped according to the trajectory clusters, and finally statistics for each group of data are listed in Table 4. Clusters 1, 2, and 7 represent relatively low and slow-moving air parcels containing high SO<sub>2</sub>, CO, and NO<sub>y</sub> concentrations, low O<sub>3</sub> concentration, accompanied by low wind speed. These three clusters of trajectories constitute 52.4 % of the total number of trajectories. The other four clusters represent air parcels mainly from the northwest or from the north. Air parcels associated with these clusters of trajectories originated from clean regions and travelled quickly at higher altitudes to Beijing. Therefore, they contained lower concentrations of SO<sub>2</sub>, CO, and NO<sub>y</sub> but higher concentration of O<sub>3</sub>. These results are consistent with those according to the analysis by surface wind directions. Cluster 4 represents air parcels moving quickest along the highest trajectory height and indicates intrusion of free tropospheric air masses. Consequently, this

**Table 4.** Trajectory clusters and their corresponding mean pollutants concentrations, travelling height, and surface wind speed.

	Clu1	Clu2	Clu3	Clu4	Clu5	Clu6	Clu7
Num	62	113	39	65	88	46	87
Ratio	12.4 %	22.6 %	7.8 %	13.0 %	17.6 %	9.2 %	17.4 %
Height (m)	407	41	894	1004	756	653	47
O <sub>3</sub> (ppb)	7.2	5.1	21.2	21.7	16.8	11.7	6.1
CO (ppm)	2.37	3.02	1.01	0.74	0.97	1.80	3.01
SO <sub>2</sub> (ppb)	42.1	53.4	12.6	9.7	16.5	28.7	43.0
NO (ppb)	42.1	53.4	11.0	4.8	9.7	28.9	40.6
NO <sub>2</sub> (ppb)	40.9	50.9	17.7	15.8	22.2	32.7	40.3
NO <sub>x</sub> (ppb)	83.0	104.3	28.7	20.6	31.9	61.5	80.9
NO <sub>z</sub> (ppb)	10.8	17.7	4.3	2.3	3.3	8.9	15.9
NO <sub>y</sub> (ppb)	93.8	122.1	32.9	22.9	35.2	70.4	96.8
WS (m s <sup>-1</sup> )	1.4	1.3	2.9	3.0	2.4	2.2	1.1

**Fig. 8.** The mean trajectories for the trajectory clusters and their ratios to the total number of trajectories.

cluster is associated with the highest concentration of O<sub>3</sub> (~22 ppb) and the lowest concentrations of SO<sub>2</sub>, CO, and NO<sub>y</sub>. In the case study above, most trajectories for the clean period from 28 December 2007 to 1 January 2008 belong to cluster 4. Cluster 3 has the similar characteristics as cluster 4, but it seemed to travel along more polluted areas.

Some earlier studies show that dry air masses with higher O<sub>3</sub> levels are linked to stratospheric air descending to lower troposphere, particularly to the high-altitude sites (Stohl et al., 2000; Gerasopoulos et al., 2001). We explored this possibility by extending the trajectory time to 120 h. The results show that most airmasses associated with higher O<sub>3</sub> and low humidity were mainly transported from the free troposphere (below 3500 m above ground level) over East Europe to the

surface layer of Beijing and no evidence for airmasses directly from stratosphere.

### 3.5 Photochemical aging and ozone production efficiency

Due to low intensity of UV radiation, photochemistry in Beijing is largely weakened in winter. Nevertheless, to some degree photochemical reactions can still take place even in the winter mixing layer. The extent of photochemistry can be expressed by photochemical age, which can be estimated using some indicators such as NO<sub>x</sub>/NO<sub>y</sub> (Parrish et al., 1992; Chameides et al., 1992; Carpenter et al., 2000; Nunnermacker et al., 1998). The air masses with very fresh emissions will have NO<sub>x</sub>/NO<sub>y</sub> close to 1, while the photochemical aged air masses have lower NO<sub>x</sub>/NO<sub>y</sub>. In this study, the average diurnal NO<sub>x</sub>/NO<sub>y</sub> varies in the range of 0.7–1, indicating that photochemical conversion of NO<sub>x</sub> is not absent but fairly slow. Therefore, the high contribution of local emission to observed NO<sub>x</sub> in winter Beijing is expected. In addition, due to declined oxidation of NO<sub>x</sub> in winter, air masses transported from far away may also have higher NO<sub>x</sub>/NO<sub>y</sub>. To make the inference more robust, we calculated the NO<sub>x</sub>/NO<sub>y</sub> and NO/NO<sub>y</sub> ratios for higher and lower wind speeds. For wind speeds lower than 2 m s<sup>-1</sup>, the NO<sub>x</sub>/NO<sub>y</sub> and NO/NO<sub>y</sub> ratios are 0.87 and 0.44, respectively; for wind speeds higher than 4 m s<sup>-1</sup>, the ratios are 0.81 and 0.16, respectively. According to Table 4 and Fig. 8, NO<sub>x</sub>/NO<sub>y</sub> (NO/NO<sub>y</sub>) is 0.90 (0.21) for the longest trajectory cluster (clu 4), and 0.85 (0.44) and 0.84 (0.42) for the two shortest trajectory clusters (clu 2 and clu 7, respectively). It seems that for the urban site in Beijing, the NO<sub>x</sub>/NO<sub>y</sub> ratio of long-range transported air is not much lower than that of local air. This may reflect the fact that the photochemical conversion of NO<sub>x</sub> in winter is at minimum in Beijing and its surrounding areas. However, long-range transport or stronger wind speed promotes the vertical mixing of O<sub>3</sub> and enhances the O<sub>3</sub> level

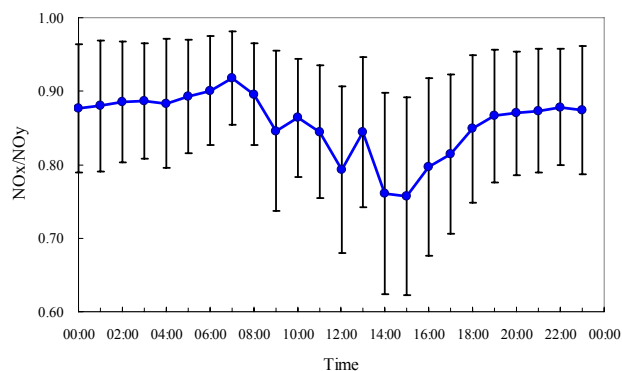


**Fig. 9.** The average diurnal variation of  $\text{NO}_x/\text{NO}_y$  ( $\pm 1\sigma$  for error bar).

(as shown in Table 4), which helps the conversion of surface NO to  $\text{NO}_2$ . This leads to much lower  $\text{NO}/\text{NO}_y$  ( $\leq 0.21$ ) for long-range transported air compared to local air. For the whole dataset, the average  $\text{NO}/\text{NO}_y$  is 0.40, which is close to the value for lower wind condition and nearly twice of that for long-range transport condition. In addition, long-range transported air masses in winter Beijing are mainly from the northwest sector and contain much lower  $\text{NO}_x$  as shown in Table 4 and Fig. 7, hence can dilute the  $\text{NO}_x$  concentration in local air of Beijing. Therefore, local sources contribute most of the ambient  $\text{NO}_x$  in urban Beijing in winter.

Figure 9 shows the average diurnal change of  $\text{NO}_x/\text{NO}_y$  during the observation period. The values of  $\text{NO}_x/\text{NO}_y$  in daytime were lower than that in nighttime because photochemical conversion of  $\text{NO}_x$  is expected in daytime. The maximum (0.92) appeared at 07:00 LT and the minimum (0.76) appeared at 15:00 LT when  $\text{O}_3$  concentration also peaked (see Fig. 5). The minimum value of 0.76 is still higher than a value of 0.6, suggesting that the air masses were not aging enough and influenced significantly by fresh urban emissions (Nunnermacker et al., 1998).

The simultaneous measurements of  $\text{O}_3$ ,  $\text{NO}_x$ , and  $\text{NO}_y$  provide an opportunity to calculate the ozone production efficiency (OPE) under the winter conditions in a megacity. From the data of  $\text{O}_x$  ( $\equiv \text{O}_3 + \text{NO}_2$ ) and  $\text{NO}_z$ , the ratio of  $\Delta(\text{O}_z)/\Delta(\text{NO}_z)$  can be calculated and considered to be a kind of observation-based OPE (Olszyna et al., 1994; Sillman, 2000; Trainer et al., 1993; Kleinman et al., 2002; Nunnermacker et al., 1998). Figure 10 shows the time series of daily OPE<sub>x</sub> during the observation period. Daily OPE<sub>x</sub> values are calculated using the  $\text{NO}_z$  and  $\text{O}_x$  data between 07:00–11:00 LT: The OPE<sub>x</sub> values are in the range of 0–8.9 ( $\text{ppb ppb}^{-1}$ ) with the mean ( $\pm 1\sigma$ ) and median values being 1.1 ( $\pm 1.6$ ) and 0.5 ( $\text{ppb ppb}^{-1}$ ), respectively. To date, most of the reported OPE values are obtained for the warm seasons (Xu et al., 2009); winter OPE values are only available for the Harvard Forest site (Hirsch et al., 1996) and the Alps site (Zanis et al., 2007). The mean value of 1.1 can be considered as the aver-

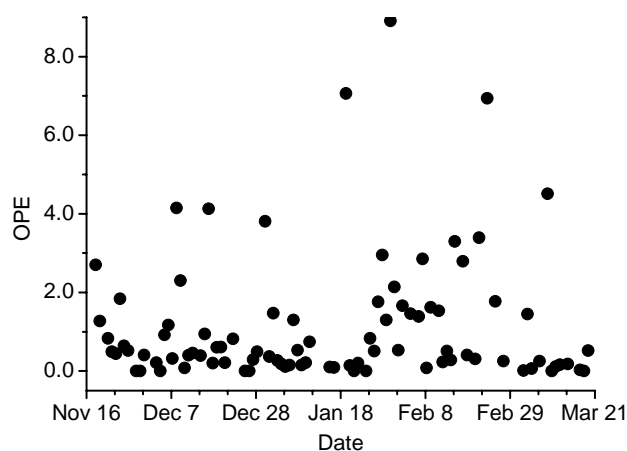


**Fig. 10.** Time series of daily OPE<sub>x</sub> during the observation period for the CMA site. Daily OPE<sub>x</sub> values are calculated using the  $\text{NO}_z$  and  $\text{O}_x$  data between 07:00–11:00 LT. The OPE<sub>x</sub> values are in the range of 0–8.9 ( $\text{ppb ppb}^{-1}$ ) with the mean ( $\pm 1\sigma$ ) and median values being 1.1 ( $\pm 1.6$ ) and 0.5 ( $\text{ppb ppb}^{-1}$ ), respectively.

age OPE<sub>x</sub> in winter for an urban site in the megacity Beijing. This winter OPE<sub>x</sub> value is much smaller than the reported OPE<sub>x</sub> values of 3.9–9.7 in summer (Chou et al., 2009) and 1.5–6.0 in fall (An, 2006) for Beijing. The smaller winter OPE value in Beijing could be due to the weaker photochemistry and higher  $\text{NO}_x$  concentration. At high  $\text{NO}_x$  concentrations, OPE tends to decrease with the increase of the  $\text{NO}_x$  concentration (Kleinman et al., 2002; Ge et al., 2010). In the megacities like Beijing, the  $\text{NO}_x$  level is usually much higher than needed for photochemical  $\text{O}_3$  production. Excessive  $\text{NO}_x$  causes net  $\text{O}_3$  loss rather than accumulation. About 27% of daily OPE<sub>x</sub> are negative, implying consumption of  $\text{O}_3$  by excessive  $\text{NO}_x$ . Such  $\text{O}_3$  loss due to high  $\text{NO}_x$  was also observed at the rural site Gucheng in the North China Plain (Lin et al., 2009). Taking the average OPE of 1.1 and the average daytime enhancement of  $\text{NO}_z$  (about 5 ppb), one can obtain an average photochemical  $\text{O}_3$  production of about 5 ppb. This is a small but significant source for surface  $\text{O}_3$  in winter in Beijing.

## 4 Conclusions

Major gaseous pollutants were observed at an urban site in the megacity Beijing during the heating period 2007–2008. The average concentrations (with  $\pm 1\sigma$ ) of NO,  $\text{NO}_2$ ,  $\text{NO}_x$ ,  $\text{NO}_y$ , CO,  $\text{SO}_2$ , and  $\text{O}_3$  were  $29.0 \pm 2.7$  ppb,  $33.7 \pm 1.4$  ppb,  $62.7 \pm 4.0$  ppb,  $72.8 \pm 4.5$  ppb,  $1.99 \pm 0.13$  ppm,  $31.9 \pm 2.0$  ppb, and  $11.9 \pm 0.8$  ppb, respectively, and the daily mean concentrations of these gases peaked at 129.6 ppb, 81.0 ppb, 210.5 ppb, 234.8 ppb, 8.71 ppm, 97.6 ppb, and 31.7 ppb, respectively. The average ratio  $\text{NO}_x/\text{NO}_y$  was  $0.86 \pm 0.10$ , suggesting that the gaseous pollutants in Beijing in winter

are mainly from local fresh emissions. The levels of the pollutants observed in this study were much lower than those reported for previous winter periods, indicating that pollution control measures adopted by the Beijing municipal government had effectively reduced emissions of gaseous pollutants. However, there is no reason to be optimistic about the air quality in Beijing. Although the SO<sub>2</sub> level has largely decreased and may decrease further, the NO<sub>x</sub> level may continue to rise with expected increase in the vehicle number. Further efforts are necessary to reduce emissions, particularly that of NO<sub>x</sub>.

Gaseous pollutants in Beijing showed large (one to two orders of magnitude) variability in the winter concentrations. The concentration time series of the pollutants display “saw-toothed” patterns. Such patterns of variation are tightly related to meteorological conditions, particularly wind direction and speed. Periodic changes in synoptic systems cause strong variations in wind direction and speed. Because of the inhomogeneous topography and source distributions in Beijing and surrounding areas, different winds exert different influences on the concentrations of pollutants. Northwest to north winds, which are normally very strong in winter, lead to much lower concentrations of primary pollutants and the opposite winds lead to accumulation of the pollutants in the surface layer. The level of surface O<sub>3</sub> during winter in Beijing urban area is normally very low due to the chemical destruction by high NO. Under strong northwest to north winds, however, it may be elevated by downward transport of O<sub>3</sub>-rich air from the free troposphere. These factors helped the formation of two types of background levels of trace gases. The background levels of CO, SO<sub>2</sub>, NO<sub>y</sub>, and O<sub>3</sub> are differentiated by decomposing the frequency distribution of the hourly average concentration of each gas into two Lorentz curves. The background levels of CO, SO<sub>2</sub>, NO<sub>y</sub>, and O<sub>3</sub> in winter Beijing under the relatively clean conditions are about 716 ppb, 5.5 ppb, 15.6 ppb, and 23.2 ppb, respectively, while those under the polluted conditions are about 2130 ppb, 20.4 ppb, 52.1 ppb, and 0 ppb, respectively.

The concentrations of primary pollutants showed similar diurnal cycles with early morning and midnight peaks and broad valley in the afternoon. The concentrations of SO<sub>2</sub>, CO, and NO<sub>x</sub> (NO<sub>y</sub>) were highly significantly correlated among each other. The correlations can be attributable to the common sources and mixing processes. The observation site is influenced by point and mobile sources. While both types of the sources are nearly equally important for NO<sub>y</sub>, they are of very different importance for CO and SO<sub>2</sub>, with mobile sources emitting much more CO than SO<sub>2</sub>, and point sources emitting much more SO<sub>2</sub> than CO. These emission differences facilitate the study of relative contributions to NO<sub>y</sub> from point and mobile sources. For this, multiple-linear regression analysis is applied to daytime, nighttime, and all data measurements and empirical equations are obtained for different datasets. Based the equations and observed winter concentrations of CO and SO<sub>2</sub>, the relative contributions

from mobile and point sources to NO<sub>y</sub> is estimated to be  $66 \pm 30\%$  and  $40 \pm 16\%$ , respectively. These figures suggest that even in the heating period, mobile sources in Beijing contribute more to NO<sub>y</sub> than point sources. Therefore, reducing emissions from mobile sources should be given priority to fight air pollution, particularly photochemical smog.

Photochemical production of O<sub>3</sub> in the winter mixing layer in Beijing is largely reduced due to much weaker photochemistry. However, the observed diurnal variations of O<sub>3</sub>, NO<sub>z</sub>, and NO<sub>x</sub>/NO<sub>y</sub> indicate that photochemistry in Beijing is perceivable even in the cold winter period. Based on the O<sub>3</sub> and NO<sub>z</sub> data, the OPE is estimated to be in the range of 0–8.9 (ppb ppb<sup>-1</sup>) with the mean ( $\pm 1\sigma$ ) and median values being  $1.1(\pm 1.6)$  and  $0.5$  (ppb ppb<sup>-1</sup>), respectively, for the winter 2007–2008 in Beijing. This low OPE, together with the small average daytime enhancement of NO<sub>z</sub>, would cause a photochemical O<sub>3</sub> source of  $5$  ppb day<sup>-1</sup>, which is small but significant for surface O<sub>3</sub> in winter in Beijing.

*Acknowledgements.* This work is supported by the National Natural Science Foundation of China (40775074, 40475046), the Basic Research Fund of CAMS (2008Z011 and 2011Z003) and of CMA (GYHY[QX]200706005).

Edited by: X. Tie

## References

- AMS: The Glossary of Meteorology (<http://amsglossary.allenpress.com/glossary>), American Meteorological Society, 2000.
- An, J. L.: Ozone production efficiency in Beijing area with high NO<sub>x</sub> emissions (in Chinese with English abstract), *Acta Scientiae Circumstantiae*, 26(4), 652–657, 2006.
- An, J. L., Wang, Y., Li, X., Lou, S., Yin Yan, and Shen, S.: Measurement on the Atmospheric SO<sub>2</sub>, NO<sub>x</sub>, CO and O<sub>3</sub> concentrations in Beijing, *Ecol. Environ.*, 16(6), 1585–1589, 2007 (in Chinese with English abstract).
- An, J. L., Wang, Y., Li, X., Sun, Y., and Shen, S.: Analysis of relationship between CO and wind-speed in Beijing, *Ecol. Environ.*, 17(1), 153–157, 2008 (in Chinese with English abstract).
- Atkinson, R., Baulch, D. L., Cox, R. A., Hampson, R. F. J., Kerr, J. A., Rossi, M. J., and Troe, J.: Evaluated kinetic and photochemical data for atmospheric chemistry: supplement VI. IUPAC subcommittee on gas kinetic data evaluation for atmospheric chemistry, *J. Phys. Chem. Ref. Data*, 26, 1329–1499, 1997.
- Carpenter, L. J., Green, T. J., Mills, G. P., Bauguutte, S., Penkett, S. A., Zanis, P., Schuepbach, E., Schmidbauer, N., Monks, P. S., and Zellweger, C.: Oxidized nitrogen and ozone production efficiencies in the springtime free troposphere over the Alps, *J. Geophys. Res.* 105, 14547–14559, 2000.
- Chameides, W. L., Fehsenfeld, F., Rodgers, M. O., Cardelino, C., Martinez, J., Parrish, D., Lonneman, W., Lawson, D. R., Rasmussen, R. A., Zimmerman, P., Greenberg, J., Middleton, P., and Wang, T.: Ozone precursor relationships in the ambient atmosphere, *J. Geophys. Res.*, 97, 6037–6055, 1992.
- Chou, C. C.-K., Tsai, C. Y., Shiu, C. J., Liu, S. C., and Zhu, T.: Measurement of NO<sub>y</sub> during Campaign of Air Quality Research in

- Beijing 2006 (CAREBeijing-2006): Implications for the ozone production efficiency of  $\text{NO}_x$ , *J. Geophys. Res.*, 114, D00G01, doi:10.1029/2008JD010446, 2009.
- Ding, G., Meng, Z., Yu, H., Wang, S., Wen, D., and Wang, X.: Measurement and research on ABL air pollution in Beijing (in Chinese with English abstract), *J. Appl. Meteorol. Sci.*, 13, 82–91, 2002.
- Gerasopoulos, E., Zanis, P., Stohl, A., Zerefos, C. S., Papastefanou, C., Ringer, W., Tobler, L., Hübener, S., Gäggeler, H. W., Kanter, H. J., Tositti, L., and Sandrini, S.: A climatology of  $^7\text{Be}$  at four high-altitude stations at the Alps and the Northern Apennines, *Atmos. Environ.*, 35, 6347–6360, 2001.
- Ge, B., Xu, X., Lin, W., and Wang, Y.: Observational study of ozone production efficiency at the Shangdianzi Regional Background Station, *Environ. Sci.*, 31(7), 1444–1450, 2010 (in Chinese with English abstract).
- Hao, J., He, D., Wu, Y., Fu, L., and He, K.: A study of the emission and concentration distribution of vehicular pollutants in the urban area of Beijing, *Atmos. Environ.*, 34, 453–465, 2000.
- Hao, J., Wang, L., Li, L., Hu, J., and Yu, X.: Air pollutants contribution and control strategies of energy-use related sources in Beijing, *Science in China (Ser. D Earth Sciences)*, 48, 138–146, 2005.
- Hao, J., Wang, L., Shen, M., Li, L., and Hu, J.: Air quality impacts of power plant emissions in Beijing, *Environ. Pollut.*, 147, 401–408, 2007.
- Hirsch, A. I., Munger, J. W., Jacob, D. J., Horowitz, L. W., and Goldstein, A. H.: Seasonal variation of the ozone production efficiency per unit  $\text{NO}_x$  at Harvard Forest, Massachusetts, *J. Geophys. Res.*, 101(D7), 12659–12666, 1996.
- Kleinman, L., Daum, P. H., Lee, Y.-N., Nunnermacker, L. J., Springston, S. R., Weinstein-Lloyd, J., and Rudolph, J.: Ozone production efficiency in an urban area, *J. Geophys. Res.*, 107, 4733, doi:10.1029/2002JD002529, 2002.
- Li, J., Qiu, Q., Xin, L., Sun, F., and Li, L.: The characteristics and cause analysis of heavy-air-pollution in Autumn and winter in Beijing (in Chinese with English abstract), *Environmental Monitoring in China*, 23, 89–94, 2007.
- Lin, W., Xu, X., Zhang, X., and Tang, J.: Contributions of pollutants from North China Plain to surface ozone at the Shangdianzi GAW Station, *Atmos. Chem. Phys.*, 8, 5889–5898, doi:10.5194/acp-8-5889-2008, 2008.
- Lin, W., Xu, X., Ge, B., and Zhang, X.: Characteristics of gaseous pollutants at Gucheng, a rural site southwest of Beijing, *J. Geophys. Res.*, 114, D00G14, doi:10.1029/2008JD010339, 2009.
- Liu, J., Zhang, X., Xu, X., and Xu, H.: Comparison analysis of variation characteristics of  $\text{SO}_2$ ,  $\text{NO}_x$ ,  $\text{O}_3$  and  $\text{PM}_{2.5}$  between rural and urban areas, Beijing (in Chinese with English abstract), *Environ. Sci.*, 29(4), 1059–1065, 2008.
- Meng, Z. Y., Xu, X. B., Yan, P., Ding, G. A., Tang, J., Lin, W. L., Xu, X. D., and Wang, S. F.: Characteristics of trace gaseous pollutants at a regional background station in Northern China, *Atmos. Chem. Phys.*, 9, 927–936, doi:10.5194/acp-9-927-2009, 2009.
- Nunnermacker, L. J., Imre, D., Daum, P. H., Kleinman, L., Lee, Y.-N., Lee, J. H., Springston, S. R., Newman, L., Weinstein-Lloyd, J., Luke, W. T., Banta, R., Alvarez, R., Senff, C., Sillman, S., Holdren, M., Keigley, G. W., and Zhou, X.: Characterization of the Nashville urban plume on July 3 and July 18, 1995, *J. Geophys. Res.*, 103, 28129–28148, 1998.
- Ohara, T., Akimoto, H., Kurokawa, J., Horii, N., Yamaji, K., Yan, X., and Hayasaka, T.: An Asian emission inventory of anthropogenic emission sources for the period 1980–2020, *Atmos. Chem. Phys.*, 7, 4419–4444, doi:10.5194/acp-7-4419-2007, 2007.
- Olszyna, K. J., Bailey, E. M., Simonaitis, R., and Meagher, J. F.:  $\text{O}_3$  and  $\text{NO}_y$  relationships at a rural site, *J. Geophys. Res.*, 99, 14557–14563, 1994.
- Parrish, D. D., Hahn, C. J., Williams, E. J., Borton, R. B., Fehsenfeld, F. C., Singh, H. B., Shetter, J. D., Gandrud, B. W., and Ridley, B. A.: Indications of photochemical histories of Pacific air masses from measurements of atmospheric trace species at Point Arena, California, *J. Geophys. Res.*, 97, 15883–15901, 1992.
- Richter, A., Burrows, J. P., Hendrik, N., Claire, G., and Ulrike, N.: Increase in tropospheric nitrogen dioxide over China observed from space, *Nature*, 437, 129–132, 2005.
- Shao, M., Tang, X., Zhang, Y., and Li, W.: City clusters in China: air and surface water pollution, *Front. Ecol. Environ.* 4, 353–361, 2006.
- Sillman, S.: Ozone production efficiency and loss of  $\text{NO}_x$  in power plant plumes: Photochemical model and interpretation of measurements in Tennessee, *J. Geophys. Res.*, 105, 9189–9202, 2000.
- Stehr, J. W., Dickerson, R. R., Hollock-Waters, K. A., Doddridge, B. G., and Kirk, D.: Observations of  $\text{NO}_y$ , CO, and  $\text{SO}_2$  and the origin of reactive nitrogen in the eastern United States, *J. Geophys. Res.*, 105, 3553–3563, 2000.
- Stohl, A., Spichtinger-Rakowsky, N., Bonasoni, P., Feldmann, H., Memmesheimer, M., Scheel, H. E., Trickl, T., Hubener, S., Ringer, W., and Mandl, M.: The influence of stratospheric intrusions on alpine ozone concentrations, *Atmos. Environ.*, 34, 1323–1354, 2000.
- Streets, D. G., Fu, J. S., Jang, C. J., Hao, J., He, K., Tang, X., Zhang, Y., Wang, Z., Li, Z., Zhang, Q., Wang, L., Wang, B., and Yu C.: Air quality during the 2008 Beijing Olympic Games, *Atmos. Environ.*, 41, 480–492, 2007.
- Tong, D. Q., Kang, D., Viney, P. A., and Rayb, J. D.: Reactive nitrogen oxides in the southeast United States national parks: source identification, origin, and process budget, *Atmos. Environ.*, 39, 315–327, 2005.
- Trainer, M., Parrish, D. D., Buhr, M. P., Norton, R. B., Fehsenfeld, F. C., Anlauf, K. G., Bottenheim, J. W., Tang, Y. Z., Wiebe, H. A., Roberts, J. M., Tanner, R. L., Newman, L., Bowersox, V. C., Meagher, J. F., Olszyna, K. J., Rodgers, M. O., Wang, T., Berresheim, H., Demerjian, K. L., and Roychowdhury, U. K.: Correlation of  $\text{O}_3$  with  $\text{NO}_y$  in photochemically aged air, *J. Geophys. Res.*, 98, 2917–2925, 1993.
- van der A, R. J., Eskes, H. J., Boersma, K. F., van Noije, T. P. C., Van Roozendaal, M., De Smedt, I., Peters, D. H. M. U., and Meijer, E. W.: Trends, seasonal variability and dominant  $\text{NO}_x$  source derived from a ten year record of  $\text{NO}_2$  measured from space, *J. Geophys. Res.*, 113, D04302, doi:10.1029/2007JD009021, 2008.
- Wang, T., Cheung, T., Li, F. Y. S., Yu, X. M., and Blake, D. R.: Emission characteristics of CO,  $\text{NO}_x$ ,  $\text{SO}_2$  and indications of biomass burning observed at a rural site in eastern China, *J. Geophys. Res.*, 107(D12), 4157, doi:10.1029/2001JD000724, 2002.
- Wang, T., Ding, A., Gao, J., and Wu, W. S: Strong ozone production in urban plumes from Beijing, China, *Geophys. Res. Lett.*, 33,

- L21806, doi:10.1029/2006GL027689, 2006.
- Xu, X., Ge, B., and Lin, W.: Progress in the research of ozone production efficiency (OPE), *Adv. Earth Sci.*, 24(8), 845–853, 2009 (in Chinese with English abstract).
- Zanis, P., Ganser, A., Zellweger, C., Henne, S., Steinbacher, M., and Staehelin, J.: Seasonal variability of measured ozone production efficiencies in the lower free troposphere of Central Europe, *Atmos. Chem. Phys.*, 7, 223–236, doi:10.5194/acp-7-223-2007, 2007.
- Zhang, J., Miao, H., Ouyang, Z. Y., and Wang, X.: Ambient air quality trends and driving factor analysis since 1980's in Beijing (in Chinese with English abstract), *Acta Scientiae Circumstantiae*, 26(11), 1886–1892, 2006.
- Zhang, Q., Streets, D. G., Carmichael, G. R., He, K. B., Huo, H., Kannari, A., Klimont, Z., Park, I. S., Reddy, S., Fu, J. S., Chen, D., Duan, L., Lei, Y., Wang, L. T., and Yao, Z. L.: Asian emissions in 2006 for the NASA INTEX-B mission, *Atmos. Chem. Phys.*, 9, 5131–5153, doi:10.5194/acp-9-5131-2009, 2009.
- Zhang, R., Cao, J., Lee, S., Shen, Z., and Ho, K.: Carbonaceous aerosols in PM10 and pollution gases in winter in Beijing, *J. Environ. Sci.*, 19, 564–571, 2007a.
- Zhang, X., Zhang, P., Zhang, Y., Li, X., and Qiu, H.: The trend, seasonal cycle, and sources of tropospheric NO<sub>2</sub> over China during 1997–2006 based on satellite measurement, *Science in China (Series D: Earth Sciences)*, 50(12), 1877–1884, 2007b.